

# Spatial Constraint Corrections to the Elasticity of dsDNA Measured with Magnetic Tweezers.

C. Bouchiat

*Laboratoire de Physique Théorique de l'Ecole Normale Supérieure*

*24, rue Lhomond, F-75231 Paris Cedex 05, France.*

(Dated: October 29, 2018)

## Abstract

In the present paper, we have studied a discrete version of the WLC model, which incorporates the spatial constraints imposed by the magnetic tweezer, used in current micro-manipulation experiments. These obstruction effects are relevant for “short” molecules, involving about two thousand base pairs or less. Two elements of the device have to be considered: first, the fixed plastic slab on which is stuck one molecule end, second, a magnetic bead which is used to pull (or twist) the attached molecule free end. We have developed quantitative arguments showing that the bead surface can be replaced by its tangent plane at the anchoring point, when it is close to the bead south pole relative to the pulling direction. We are, then, led to a confinement model involving two repulsive plates: first, the fixed anchoring plate, second, a fluctuating plate, simulating the bead, in thermal equilibrium with the attached molecule and the ambient fluid. The bead obstruction effect reduces to a slight upper shift of the elongation, about four times smaller and with the same sign as the effect induced by the anchoring plate. This result, which may contradict naive expectations, has been qualitatively confirmed within the soluble “Gaussian” model for flexible polymers. A study of the molecule elongation versus the contour length  $L$  exhibits a significant non-extensive behavior. Although the curve for “short” molecules is well fitted by a straight line, with its slope very close to the prediction of the standard WLC model, it does not pass through the origin, due the presence of an offset term independent of  $L$ . This leads to a 15% upward shift of the elongation for a 2 kbp molecule. Finally, the need for thorough analysis of the spatial constraints in super-coiled dsDNA elasticity measurements is illustrated by “hat” curves, giving the elongation versus the torque.

PACS numbers: 87.15.By, 61.41+e

## I. INTRODUCTION

In the last decade, single particle biophysics has developed into a very active field of research [1, 2, 3, 4, 5]. In particular, micro-manipulation experiments are now recognized as valuable tools to observe, in real time, a single double-strand DNA (dsDNA) molecule interacting with the proteins involved in the cell duplication processes. The basic principle is to look for sudden variations of the stretched dsDNA molecule elongation, which occur when the biochemical reaction is taking place. (For two recent reviews see the references [1, 2].)

In recent experiments [6, 7], there is a tendency to use relatively short segments with 2000 base pairs (2 kbp), corresponding to  $L \simeq 680$  nm; this number is to be compared with the persistence length of the dsDNA molecule  $A \simeq 50$  nm. This implies that finite size effects may be of some importance, specially the spatial obstruction caused by magnetic tweezers.

The simplest way to implement spatial constraints is to introduce in the dsDNA elastic energy density a one-monomer potential  $V(\mathbf{r}(s))$ , where  $\mathbf{r}(s)$  is the coordinate of the monomer, running along the chain of arc-length  $s$ . The “worm-like-chain” (WLC) model [8, 9, 10] describes rather accurately dsDNA elongation experiments. In its usual formulation, the sole dynamical variable is the running tangent vector  $\mathbf{t}(s) = \frac{d}{ds} \mathbf{r}(s)$  and in that case, one has to write  $\mathbf{r}(s) = \int_0^s \mathbf{t}(s') ds'$ . The potential energy to be added to  $E_{WLC}$  takes then an ugly non local form  $\int_0^L ds V(\int_0^s \mathbf{t}(s') ds')$ . This difficulty can be solved by formulating the model in such a way that  $\mathbf{t}(s)$  and  $\mathbf{r}(s)$  behave as independent dynamical variables.

Numerous authors addressed this problem within the continuous version of the WLC model. The statistical properties of the molecular chain are obtained by solving a Quantum Mechanics problem, involving an imaginary time  $-i s$ . Using various arguments, they found that the Hamiltonian, allowing for spatial constraints, is obtained by adding two extra terms to the standard WLC Hamiltonian  $H_{WLC} = -\frac{1}{2A} \nabla_{\mathbf{t}}^2 - \mathbf{t} \cdot \mathbf{f}$ . ( $\mathbf{f}$  is the stretching force given in thermal units.) The first is the so-called “ballistic” term  $\nabla \cdot \mathbf{t}$  and the second is the potential  $V(\mathbf{r})$  [14, 15, 16, 17, 18, 19, 20, 21, 22, 23, 24]. This model has been applied to various problems in semi-flexible polymer physics: the flow of semi-flexible polymers through cylindrical pores [18], the unbinding transition between semi-flexible polymers attracted by directed polymers [19], the symmetric interface between two immiscible semi-flexible polymers [24] and probably others...

In reference [13], we have taken a different approach by remaining within a discrete version of the WLC model, which has to be introduced anyhow, if one wants to write down explicitly the functional integral giving the Boltzmann partition function. By using a simple trick, we were able to write the partition function as a multiple integral, where the coordinates  $\mathbf{r}_n$  and the tangent vectors  $\mathbf{t}_n$  of the discrete molecular chain are treated as independent integration variables. Using the transfer matrix formalism, it is then possible to write down a recurrence relation between adjacent intermediate partition functions  $Z_n(\mathbf{r}_n, \mathbf{t}_n)$  relative to chains having a crystallographic length smaller than the actual one:

$$Z_{n+1}(\mathbf{r}_{n+1}, \mathbf{t}_{n+1}) = \exp(-bV(\mathbf{r}_{n+1})) \int d^2\Omega(\mathbf{t}_n) T_{WLC}(\mathbf{t}_{n+1} | \mathbf{t}_n) Z_n(\mathbf{r}_{n+1} - b\mathbf{t}_{n+1}, \mathbf{t}_n), \quad (1)$$

where  $T_{WLC}(\mathbf{t}_{n+1} | \mathbf{t}_n)$  is the transfer matrix relative to the unconstrained WLC model. All the explicit computations performed in reference [13] and in the present paper are based upon the above iterative construction, which has a suggestive interpretation in terms of a Markov random walk model in three dimensions.

The confined dsDNA configurations studied in reference [13] were not fully realistic, since they do not account properly for the spatial obstructions occurring in magnetic tweezers. To get a feeling about the orders of magnitude involved in “short” molecules, say with  $L \lesssim 10 A$ , let us quote the results obtained in ref. [13] for the relative elongation upward shifts induced by the spatial obstruction of the anchoring plate. ( By anchoring plate, we mean the plastic slab upon which is stuck the initial molecular strand with the help of a “biological glue”.) For a typical stretching force  $F \simeq 0.3$  pN, the upward shift is given by  $1.6 A/L$ , which amounts to 12 % for a 2 kbp molecule. In a magnetic tweezer, the free end of the dsDNA molecule is attached to a magnetic spherical bead, having a diameter of about one micron. In view of the above result, the bead obstruction effects are certainly worth investigating. (To get a very schematic view of the various constrained and unconstrained situations to be studied in the present work, see the upper graph of Fig.2 .) Such a study will be particularly relevant for dsDNA molecules with a few kbp, when they are stretched by forces within the range 0.1 to 0.5 pN.

A theoretical analysis of the spatial obstructions in a magnetic tweezer is a difficult task, if one wants to treat it as a full three-dimension space problem, within the WLC model. The difficulties are about the same in the approaches based upon the solving of a Schrödinger-like equation or the transfer matrix iteration technique. The Monte-Carlo

method, which could perhaps be a viable approach, will not be considered in this paper because of lack of competence of the author. We are going to temper the above pessimistic views, by showing that under well defined conditions the nucleotides do not really feel the curvature of the bead. More precisely, the bead surface can be reasonably approximated by its tangent plane at the molecule free-end anchoring point, assumed to be the lowest point of the bead with respect to the force direction. It follows, then, that under realistic experimental conditions, the magnetic-tweezer obstruction can be simulated by two repulsive plates, normal to the stretching forces. There is, however, an important difference with the two-fixed-plate problem we have studied previously [13]. The initial molecular segment is still anchored to a fixed plate but the free end is now attached to a plate which is no longer fixed, but in thermal equilibrium with the dsDNA molecule and the ambient fluid. We are back to a one-dimension space iteration problem within transfer matrix technique. It is definitely more difficult than the two-fixed-plate problem but still manageable.

Volume-exclusion effects in tethered-molecule experiments have been studied recently by Monte-Carlo techniques [25]. The authors have considered the situation where no stretching force are applied upon the bead. So, their significant work cannot be compared with the present one, since we are dealing with stretched molecules, having a relative elongation larger than 0.65. A finite-size effect analysis appears also in connection with the entropic elasticity of DNA molecule, having a permanent kink [26]. In particular, the authors deal with the boundary conditions to be satisfied by the tangent vectors at the two ends of the molecular chain. In the present work, we have concentrated on the spatial confinement, imposed upon the internal monomers, by the repulsive surfaces holding the two free ends. It is easily seen that these constraints insure that the initial and terminal tangents vectors do satisfy automatically the “half-constrained” boundary conditions of ref.[26].

## **II. A SIMPLIFIED MODEL TO DESCRIBE THE MAGNETIC BEAD SPATIAL OBSTRUCTION.**

In this section, we would like to develop arguments to justify the replacement of the bead surface by its tangent plane at the anchoring point, assumed to be located at the bead south pole with respect to the force direction. The discussion will be performed within a discrete version of the WLC model. The molecular chain is represented by  $N$  elementary

links, involving point-like “effective” monomers, separated by a length  $b$ , much smaller than the persistence length  $A$ . The effective monomer number  $N$  is related to the contour length  $L$  by the relation  $N = L/b$ . A microscopic state of our model is then defined by the set of  $2N$  vector variables:  $\{(\mathbf{r}_1, \mathbf{t}_1) \dots (\mathbf{r}_n, \mathbf{t}_n), \dots (\mathbf{r}_N, \mathbf{t}_N)\}$  with  $1 \leq n \leq N$ , where  $\mathbf{r}_n$  and  $\mathbf{t}_n$ , are respectively the monomer coordinate and the unit tangent vector such that  $b \mathbf{t}_n = \mathbf{r}_n - \mathbf{r}_{n-1}$ . In this paper the  $z$  axis is parallel to the direction of the stretching force  $\mathbf{F}$  and has its origin at the fixed-plate anchoring point. One must stress that the variables  $\mathbf{r}_N$  and  $\mathbf{r}_n$  with  $1 \leq n \leq N - 1$  have to be treated on different footing:  $\mathbf{r}_N$  is the coordinate of the terminal monomer but it gives also the position of the bead.

We shall, first, discuss the transverse fluctuations of the terminal monomer,  $\langle x_N^2 \rangle$ ; they are given in the thermodynamic limit  $L/A \gg 1$  by a well known formula [5] :

$$\langle x_N^2 \rangle = \langle z_N \rangle (k_B T) / F = \frac{\langle z_N \rangle}{\alpha} A , \quad (2)$$

where  $\alpha$  is the dimensionless force parameter  $F A / (k_B T)$ . This formula is used to calibrate the force in magnetic tweezer experiments and was first obtained by a simple thermodynamic argument [5]. In an unpublished note [11], we have given a statistical mechanics evaluation of  $\langle x_N^2 \rangle$  within the WLC Model. We have recovered the formula (2) in the limit  $L/A \gg 1$  with corrections of the order of  $A/L$ , which cannot be totally ignored for the “short” molecules considered in the present paper. For this reason, we have given an updated version of this note in the appendix. The above value of  $\langle x_N^2 \rangle$  will be used as a benchmark in our estimate of the transverse fluctuations of the internal monomers. To proceed it is convenient to introduce cylindrical coordinates for the effective monomer positions  $\mathbf{r}_n = (z_n, \mathbf{r}_{\perp n})$  and the associated tangent vector  $\mathbf{t}_n = (\cos \theta_n, \mathbf{t}_{\perp n})$ . Our purpose is now to estimate the thermal average of the square of the transverse distance between the  $n$ -monomer and terminal monomer:  $\langle (\mathbf{r}_{\perp n} - \mathbf{r}_{\perp N})^2 \rangle$ . More precisely we are going to establish the inequality:

$$\langle (\mathbf{r}_{\perp n} - \mathbf{r}_{\perp N})^2 \rangle < \langle \mathbf{r}_{\perp N}^2 \rangle = 2 \langle x_N^2 \rangle = 2 \frac{\langle z_N \rangle}{\alpha} A . \quad (3)$$

We have found convenient here to work within the WLC model in its simplest form, where only the tangent vectors  $\mathbf{t}_n = (\cos \theta_n, \cos \theta_n, \sin \theta_n \cos \phi_n, \sin \theta_n \sin \phi_n)$  appear explicitly. The  $n$ -monomer coordinate is then given by the sum:  $\mathbf{r}_n = b \sum_{i=1}^{i=n} \mathbf{t}_i$ . The discrete *WLC* model is best formulated in terms of the transfer matrix connecting two adjacent links:

$$T_{WLC}(\mathbf{t}_{n+1}, \mathbf{t}_n) \propto \exp \left( -\frac{A}{2b} (\mathbf{t}_{n+1} - \mathbf{t}_n)^2 \right)$$

$$\propto \exp\left(\frac{A}{b}(\cos\theta_{n+1}\cos\theta_n + \sin\theta_{n+1}\sin\theta_n\cos(\phi_{n+1} - \phi_n))\right), \quad (4)$$

where for simplicity we have omitted the stretching energy term. Our aim is to prove that the following difference is positive:

$$\Delta_{\perp} = \langle \mathbf{r}_{\perp N}^2 \rangle - \langle (\mathbf{r}_{\perp n} - \mathbf{r}_{\perp N})^2 \rangle = \langle \mathbf{r}_{\perp n}^2 \rangle + 2 \sum_{i=n+1}^{i=N} \sum_{j=1}^{j=n} \langle \mathbf{t}_{\perp i} \cdot \mathbf{t}_{\perp j} \rangle. \quad (5)$$

Clearly, we have to show that the thermal average:  $\langle \mathbf{t}_{\perp i} \cdot \mathbf{t}_{\perp j} \rangle = \langle \sin\theta_i \sin\theta_j \cos(\phi_i - \phi_j) \rangle$  is positive. Within the usual definition of the cylindrical coordinates,  $\sin\theta_i \sin\theta_j$  takes only positive values while  $\cos(\phi_i - \phi_j)$  can be negative as well as positive. To prove the positivity of  $\langle \mathbf{t}_{\perp i} \cdot \mathbf{t}_{\perp j} \rangle$ , it is then enough to perform the thermal average over the azimuthal angle  $\phi_i$ , the longitudinal components  $\cos\theta_i$  being frozen. Assuming that  $\phi_1$  is initially uniformly distributed, the overall system is invariant upon any global rotation around the z-axis, so that we can replace the set of the  $N$  variables  $\phi_i$  by the  $N - 1$  variables  $\psi_i = \phi_i - \phi_{i-1}$  with  $1 < i \leq N$ . Using the formula (4) one gets immediately the probability distribution of  $\psi_i$  :

$$P_i(\psi_i) = \exp\left(\frac{A}{b} \lambda_i \cos\psi_i\right) / (2\pi I_0(\lambda_i)) , \quad \lambda_i = \sin\theta_i \sin\theta_{i-1} > 0, \quad (6)$$

where, for convenience, we shall take  $-\pi \leq \psi_i \leq \pi$ . We have, now, everything we need to compute  $\langle \cos(\phi_i - \phi_j) \rangle$ . We first note that  $\phi_i - \phi_j$  can be easily written as a sum of  $\psi_l$  angles:

$$\phi_i - \phi_j = \phi_i - \phi_{i-1} + \phi_{i-1} - \phi_{i-2} \dots \phi_{j+1} - \phi_j = \sum_{l=j+1}^{l=i} \psi_l.$$

The average  $\langle \cos(\phi_i - \phi_j) \rangle$  is then easily performed:

$$\langle \cos(\phi_i - \phi_j) \rangle = \text{Re}\left(\prod_{l=j+1}^{l=i} \langle \exp(i\psi_l) \rangle\right) = \prod_{l=j+1}^{l=i} \langle \cos\psi_l \rangle, \quad (7)$$

$$\langle \cos\psi_l \rangle = \int_{-\pi}^{-\pi} d\psi_l P_l(\psi_l) \cos\psi_l. \quad (8)$$

By looking at the functional form of  $P_l(\psi_l)$  in eq. (6) it is easily seen that  $\lambda_l > 0$  implies  $\langle \cos\psi_l \rangle > 0$  and, as a consequence, the positivity of  $\langle \cos(\phi_i - \phi_j) \rangle$ . Since the final averaging will preserve this positivity, we can conclude from eq. (5) that  $\Delta_{\perp} > 0$ , or in a more concrete way:

$$\langle (\mathbf{r}_{\perp n} - \mathbf{r}_{\perp N})^2 \rangle < \langle \mathbf{r}_{\perp N}^2 \rangle = \frac{2\langle z_N \rangle}{\alpha} A. \quad (9)$$

Let us consider, now, an internal effective monomer going upward and crossing the tangent plane at a transverse distance  $|(\mathbf{r}_{\perp n} - \mathbf{r}_{\perp N})|$  from the south pole. The maximum vertical

distance  $\delta_{curv}$  which it can travel before hitting the bead surface is given by a simple geometrical argument:  $\delta_{curv} = (\mathbf{r}_{\perp n} - \mathbf{r}_{\perp N})^2 / (2R)$  where  $R$  is the bead radius. Performing the thermal averaging we get the final inequality:

$$\langle \delta_{curv} \rangle < \frac{\langle \mathbf{r}_{\perp N}^2 \rangle}{2R} = \frac{\langle z_N \rangle}{R\alpha} A. \quad (10)$$

The internal monomers are subjected, in the vicinity of the bead, to the chain tension force which tends to pull them towards the anchoring point. As a consequence, the above assumption of a vertical path leads to an overestimate of  $\delta_{curv}$ , so relaxing this constraint can only but strengthen the inequality of eq.(10).

In order to quantify the internal monomer ability to detect the curvature of the bead, we are going to compare  $\delta_{curv}$  to other experimental lengths. Let us begin by the average elongation:  $\langle z(N) \rangle$ . We readily obtain the inequality:

$$\langle \delta_{curv} \rangle / \langle z(N) \rangle < \frac{A}{R\alpha} = 1.25 \times 10^{-2} / R(\mu), \quad (11)$$

where we have taken  $A = 50 \text{ nm}$  and  $\alpha = 4$ , which corresponds to a stretching force  $F = 0.31 \text{ pN}$ .  $R(\mu)$  stands for the bead radius given in micron. A more significant comparison involves the mean-square longitudinal fluctuation  $\Delta z_N = \sqrt{\langle z_N^2 - \langle z_N \rangle^2 \rangle}$ . We have computed the ratio  $\Delta z_N / \langle z_N \rangle$  using a version of the WLC model incorporating the confining effect of the fixed plate holding the initial strand [13]. Taking  $\alpha = 4$  and  $L = 12A$ , we have obtained:  $\Delta z_N / \langle z_N \rangle = 0.083$ . Keeping the same value of  $L$ , we have derived upper bounds of the ratio  $\langle \delta_{curv} \rangle / \Delta z_N$ , for  $\alpha = 2, 4, 5$  respectively:

$$\langle \delta_{curv} \rangle / \Delta z_N < \frac{\langle z(N) \rangle}{\Delta z_N} \frac{A}{R\alpha} = (0.17, 0.15, 0.13) / R(\mu). \quad (12)$$

We conclude that the internal monomer mean free path above the tangent plane  $\langle \delta_{curv} \rangle$  is less than one sixth of the mean-square longitudinal fluctuation of the bead  $\Delta z_N$  when  $L = 12A$  and  $\alpha \geq 2$ . This suggests that, under such conditions, the effective internal monomers are not really able to detect the bead curvature and gives a rather strong justification for the replacement of the bead surface by its tangent plane at the anchoring point.

However, one must keep in mind that the above conclusion hinges upon the simplifying assumption that the end of the DNA molecule is stuck at the south pole of the bead. This condition will not be satisfied, unless some selection is performed among the beads. This can be done in practice by slowly rotating the magnetic tweezer around its axis. The magnetic

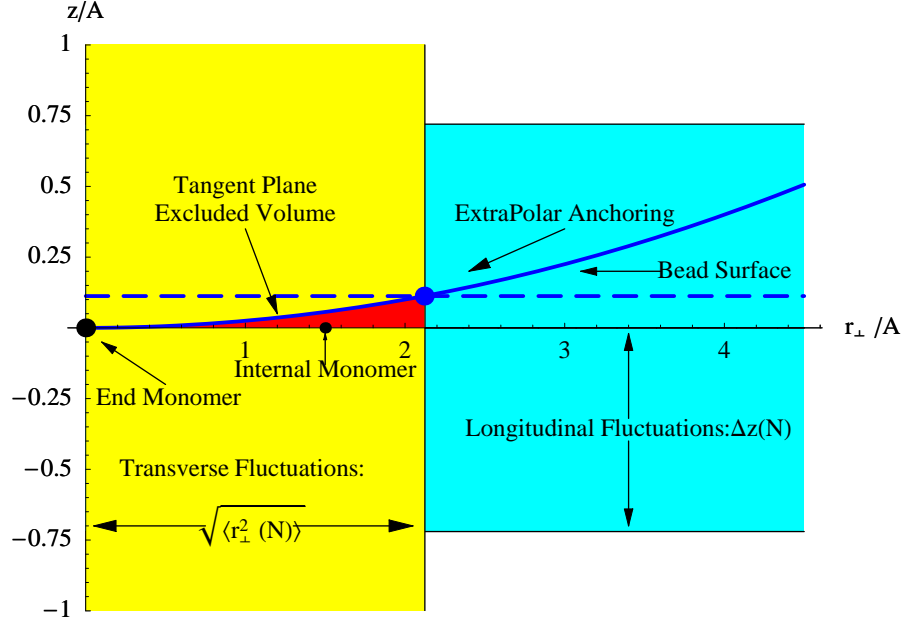


FIG. 1: A schematic picture showing the basic physical parameters governing the motion of an internal monomer (small black dot) in the vicinity of the bead surface tangent plane at the terminal monomer (big black dot) anchoring point at the south pole. The figure represents a section of the bead by a plane containing its center and parallel to the  $z$ -axis. The magnitude of the fluctuations are shown in the case of a force  $F = 0.31$  pN and a contour length  $L = 12A$ . As indicated in the text, the yellow vertical band gives an upper limit to the allowed transverse motion of an internal monomer with respect to the terminal one. The red region represents the vertical section of the excluded volume coming from the replacement of the bead surface (the blue circle arc) by its tangent plane. The emerald horizontal band gives the amplitude of the longitudinal fluctuations of the bead. A comparison with the vertical width of the red region suggests that the internal monomers will not be able to “feel” the bead curvature. The big blue dot represents the case of an anchoring point lying away from the south pole. The plane simulating the bead is now the horizontal plane  $z = z_N$  (its section appears as a blue dashed line). The excluded volume is subjected to a positive variation on the right-hand side and a negative one on the other side; so there is clearly a compensation effect. Furthermore, the selection procedure described in the text is affected by the transverse fluctuations of the bead. On this figure, we have assumed for simplicity that the selection has been performed with  $F = 0.31$  pN. Taking instead  $F = 2.7pN$  would have reduced the selection angle  $\theta_{lim}$  by a factor 3.



bead behaves as a compass and follows the rotating magnetic field. If the experiment is performed at a high enough force  $F_{selec}$ , the bead rotates around the vertical axis passing through the anchoring point lying away from the south pole ( the big blue dot appearing on Fig.1). As a consequence, the center of the bead describes a circle of radius  $R \sin \theta_{an}$ , where  $\theta_{an}$  is the “latitude” of the anchoring point with respect to the bead south pole (*i.e* the angular distance between the black point and the blue point on Fig.1). There is clearly a limitation in this bead selection procedure, coming from the transverse fluctuations of the bead. Only the beads satisfying the inequality  $\sin \theta_{an} > \sin \theta_{lim} = \sqrt{\langle \mathbf{r}_{\perp N}^2 \rangle (F/F_{selec})}/R$  can be eliminated in practice. (We have made explicit the fact that the actual elongation experiment is done at a force  $F$  different from that used in the selection procedure). Let us consider now a bead belonging to the selection. Replacing the tangent plane by the horizontal plane  $z = z_N$  induces a variation (positive or negative ) of the vertical free path of the internal monomers of amplitude smaller than  $\sin \theta_{lim} \sqrt{\langle \mathbf{r}_{\perp N}^2 \rangle} = \sqrt{F/F_{selec}} \langle \mathbf{r}_{\perp N}^2 \rangle / R$ . Taking into account the compensation apparent on Fig.1 and the eventual reduction factor  $\sqrt{F/F_{selec}}$  the average height of the excluded volume can easily be made one order of magnitude smaller than the longitudinal fluctuation of the bead  $\Delta z_N$ . Our model is then expected to be valid for the beads selected according to the above criterion.

### III. A SOLUTION OF THE MODEL AND ITS PHYSICAL INTERPRETATION.

#### A. Computation Procedure.

In this section, we are going to extend the matrix transfer method of reference [13] to the study of the statistical properties of a dsDNA molecule confined within a magnetic tweezer. The two ends of the molecule are respectively attached to a fixed plate and to a magnetic bead immersed in a liquid which simulates the cellular medium. The bead is subjected to an external force normal to the anchoring plate. This pulling force is balanced by the tension of the stretched molecule. As shown in the above section, the identification of the bead surface to its tangent plane at the terminal monomer position is a fairly good approximation if the anchoring point is close to the south pole.

Our confinement configuration is then defined by two parallel repulsive plates, the first - the anchoring plate - is fixed and the second - simulating the bead - is in thermal equilibrium

with the attached molecule and the ambient fluid. With proper initial conditions, the partition function of the system molecule-plus-bead is invariant, first, under rotations around the stretching force direction and, second, under translations parallel to the plates. We are going to use the same discrete version of the WLC model as in the previous section. A microscopic state of our model is then defined by the set of  $2N$  longitudinal variables:  $\{(z_1, \theta_1) \dots (z_n, \theta_n) \dots (z_N, \theta_N)\}$  with  $1 \leq n \leq N$ .

We proceed in two steps. We, first, assume that the terminal monomer coordinate  $z_N$  has a fixed value, taken among a finite set chosen to be representative of the actual physical spectrum. The internal monomer coordinates  $z_n$ , with  $1 \leq n \leq N - 1$ , are truly stochastic variables, associated with the partition function  $\mathcal{Z}_n(z_n, \theta_n | z_N)$ . For the moment,  $z_N$  is treated as an external physical parameter. When  $1 \leq n \leq N - 1$ , the internal partition functions  $\mathcal{Z}_n(z_n, \theta_n | z_N)$  obey a recurrence relation which is just a rewriting of a formula given in Section 2.1 of reference [13]. The rule is very simple: take the iteration equation for the fixed-plate confinement problem and identify  $z_N$  with the distance between the two repulsive plates  $L_0$ :

$$\mathcal{Z}_n(z_n, \theta_n | z_N) = \exp(-b \mathcal{V}(z_n, z_N)) \int_0^1 d(\cos \theta_{n-1}) \mathcal{T}_{WLC}(\theta_n, \theta_{n-1}, f) \times \mathcal{Z}_{n-1}(z_n - b \cos \theta_n, \theta_{n-1} | z_N). \quad (13)$$

The potential  $\mathcal{V}(z_n, z_N)$ , is written as the sum of two terms:

$$\mathcal{V}(z_N, z_n) = V_{pl}(z_n) + V_{pl}(z_N - z_n), \quad (14)$$

where the first one is associated with the fixed anchoring plate and the second with the fluctuating plate simulating the magnetic bead surface. The repulsive plate potential  $V_{pl}(z)$  is given in terms of the rounded-off step function [13]:

$$\Theta(z, \Delta z) = \frac{1}{2} + \frac{1}{2} \text{erf}(z/\Delta z), \quad (15)$$

where  $\text{erf}(x)$  is the ‘‘error’’ function :  $\frac{2}{\sqrt{\pi}} \int_0^x \exp(-t^2) dt$  and  $\Delta z$  a smoothing length assumed to be  $\sim A$ . For the sake of simplicity, it is convenient to give directly the associated Boltzmann factor:

$$\exp(-b V_{pl}(z)) = \Theta(z, \Delta z). \quad (16)$$

The conditional probability distribution  $\mathcal{T}_{WLC}(\theta_n, \theta_{n-1}, f)$  is obtained by performing an azimuthal average of the transfer matrix given by equation (4):

$$\mathcal{T}_{WLC}(\theta_1, \theta_2, f) = \exp - \left\{ \frac{A}{b} (1 - \cos \theta_1 \cos \theta_2) + \frac{b f}{2} (\cos \theta_1 + \cos \theta_2) \right\}$$

$$\times I_0\left(\frac{A \sin \theta_1 \sin \theta_2}{b}\right), \quad (17)$$

where  $f$  is related to the stretching force by  $F = f k_B T$ . We compute the partition function relative to the last internal monomer, for a fixed terminal monomer,  $\mathcal{Z}_{N-1}(z_{N-1}, \theta_n | z_N)$ , by running, up to  $n = N - 1$ , the iteration process defined by equation (13). To perform the relevant recurrence process we have used *Mathematica* codes where analytical and numerical computations are intertwined. For more details about our procedure, see the Section V of reference [29].

The second step ( a short one ! ) is to compute the partition function  $Z_N(z_N, \theta_N)$  relative to the terminal monomer. It is easily obtained from the formula:

$$Z_N(z_N, \theta_N) = \exp(-b V_{pl}(z_N)) \int_0^1 d(\cos \theta_{N-1}) \mathcal{T}_{WLC}(\theta_N, \theta_{N-1}, f) \times \mathcal{Z}_{N-1}(z_N - b \cos \theta_N, \theta_{N-1} | z_N). \quad (18)$$

Finally, the probability distribution relative to the terminal monomer longitudinal coordinate - it is also the longitudinal distance of the bead south pole from the fixed plate - is given as follows:

$$P_N(z_N) = \frac{1}{\mathcal{N}} \int_0^1 d(\cos \theta_N) Z_N(z_N, \theta_N),$$

$$\mathcal{N} = \int_0^L d(z_N) \int_0^1 d(\cos \theta_N) Z_N(z_N, \theta_N). \quad (19)$$

## B. Result and Physical Interpretation.

The probability distribution  $P_N(z_N)$  is displayed upon the left graph of Fig.2 as a continuous blue curve. It appears together with green and red curves, corresponding, respectively, to the two situations: absence of constraints and presence of a fixed anchoring plate. Two features are conspicuous:

- The red and blue curves are very close, while the green and red ones are much further apart, showing that the obstruction effect of the bead is much smaller than that coming from the fixed anchoring plate.
- Perhaps even more surprising, the bead obstruction effect reduces to a slight push upwards given to the terminal monomer, while one might have expected naively the reverse.

In the two-fixed-plate configuration studied in our previous work [13], the confinement effects upon  $P_N(z_N)$  were very spectacular ( see Figure 4. of this reference). It must be stressed that the physics involved was very different from that prevailing in the present paper. Indeed, the terminal monomer, supposed to be attached to a nano-magnet, was free to move between two diamagnetic fixed plates. When the elongation in absence of plates was larger than the two-plate distance, the probability distribution  $P_N(z_N)$  was flattened against the upper plate by the stretching force. *No such phenomenon appears here since the terminal monomer is stuck upon the plate simulating the magnetic bead. Only the internal monomers feel the repulsion of the magnetic bead and it is through their intermediary that the terminal monomer is affected by the spatial obstruction of the bead.*

A plausible mechanism goes as follows: the internal monomers are pulled upwards by the string tension force. When they collide with the bead, they are expected to give a small upward push to the bead surface. In other words, they are exerting an upward pressure on the bead, which is transmitted to the terminal monomer, leading to a small increase of the stretching force.

The positivity of the variation of the elongation  $\delta\langle z_N \rangle$  can also be obtained by a simple thermodynamic argument, valid in the limit  $\delta\langle z_N \rangle / \langle z_N \rangle \ll 1$ . The internal energy of the bead-plus-DNA system receives a positive contribution  $\delta U$  coming from the repulsive interactions:  $\sum_{n=1}^{N-1} V_{pl}(z_N - z_n) > 0$ . Writing that the variation of the free energy  $\mathcal{F} = U - \langle z_N \rangle F$  vanishes at equilibrium, one gets:  $\delta\langle z_N \rangle \simeq \delta U / F > 0$ .

In order to get a confirmation of the above picture, we have repeated our computations within the soluble ‘‘Gaussian Model’’, often used to describe ‘‘flexible’’ polymers. It involves a chain of point-like monomers connected by harmonic springs. The continuous limit of the chain is a string described by the elastic energy linear density:  $\mathcal{E}^{gaus}(s) = \frac{1}{2a} (\dot{\mathbf{r}}(s))^2 + V(\mathbf{r})$ , where  $\dot{\mathbf{r}}(s)$  is the derivative of the monomer coordinate  $\mathbf{r}(s)$  with respect to the string arc-length  $s$  and  $a^{-1}$  is proportional to the rigidity of the spring connecting nearest-neighbor monomers. The value chosen for the parameter  $a$  guarantees that the relative elongation  $af$ , in absence of spatial constraints, is the same as in the WLC model. The monomer number  $n$  is related to the arc-length  $s$  by  $s = nb$  with  $b/a \ll 1$ . If we identify  $V(\mathbf{r})$  with the potential  $\mathcal{V}(z_n, z_N)$  introduced above, the internal monomer probability distribution,  $P_n^{int}(x_n, y_n, z_n)$ , factorizes into three independent distributions relative to each component. In the continuous limit, the statistical properties of the internal monomers are easily obtained by exploiting

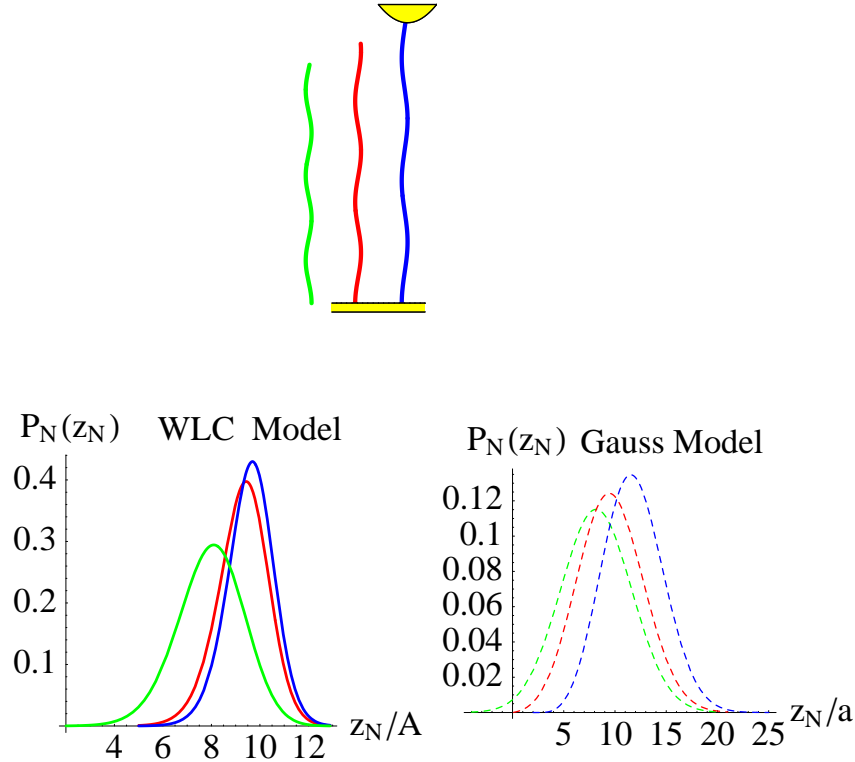


FIG. 2: Probability distributions of the terminal coordinate  $z_N$ , relative to different spatial obstruction conditions, as predicted by two models. The continuous curves appearing on the left-hand lower graph have been obtained within the WLC model, while the dashed ones on the right-hand graph are relative to the Gaussian model. As indicated in the picture given in the upper graph, the green color corresponds to a molecular chain free of any external spatial constraints. The red and blue colors are associated respectively with two kinds of spatial obstruction: restriction to the upper half space by an anchoring fixed plate and confinement between the fixed plate and the fluctuating bead, holding the terminal monomer.

the analogy with a QM problem involving the following simple Hamiltonian:

$$\widehat{H}_{int} = -\frac{a}{2} \frac{\partial^2}{\partial z_n^2} + \mathcal{V}(z_n, z_N). \quad (20)$$

The Hamiltonian relative to the terminal monomer  $\widehat{H}_{term}$  is obtained by performing the replacement :  $z_n \rightarrow z_N$  ,  $\mathcal{V}(z_n, z_N) \rightarrow V_{pl}(z_N)$ . The probability distribution for the ter-

minimal monomer involving a fixed anchoring plate together with a pulling one, in thermal equilibrium with the "Gaussian" polymer chain, reads then as follows:

$$P_N(z_N) = \int dz_{N-1} \exp(f z_N) \langle z_N | \exp(-b \widehat{H}_{term}) | z_{N-1} \rangle \langle z_{N-1} | \exp(-b(N-1) \widehat{H}_{int}) | z_0 \rangle. \quad (21)$$

The results obtained within the "Gaussian Model" are displayed on the right-hand graph of Fig.2. The obstruction effects are qualitatively similar to those obtained within the WLC model but the chain-elongation increase induced by "the bead"  $\delta \langle z_N \rangle$  is much larger. This amplification can be understood by noting that the "Gaussian flexible" monomers, being allowed to move much more freely, have a larger collision rate with "the bead".

We have studied the magnetic tweezer spatial constraint effects on the dsDNA elongation within the stretching force range defined by  $2 \leq \alpha \leq 5$ , in the case of a contour length  $L = 12 A$ . The elongation curves are displayed in Fig 3 for three configurations : no space constraints ( green line), an anchoring plate barrier ( red line) and an anchoring plate barrier together with the magnetic bead ( blue line ). As discussed above, spatial obstruction effects from the bead, in thermal equilibrium, lead to a small increase - about few %- of the elongation. It is to be compared with the four times larger effect induced by the anchoring fixed plate, where the repulsive character of the fixed barrier is clearly exhibited.

#### IV. THE NON-EXTENSIVE BEHAVIOR OF THE DNA ELONGATION IN PRESENCE OF SPATIAL CONSTRAINTS.

In this section we shall study, for fixed forces, the variation of the elongation  $\langle z(N) \rangle$  with respect to the contour length  $L$ . This analysis has been performed previously in ref. [13]. In the case of fixed plates, it was found that  $\langle z(N) \rangle$  is no longer an extensive variable with respect to  $L$ . The effects were very spectacular in the two plates configuration when the distance  $L_0$  between the two plates is smaller than the elongation in absence of spatial constraints. Conversely, when  $L_0 > L$ , the molecule feels only the anchoring plate and the extensive behavior of  $\langle z(N) \rangle$  is perturbed in a very simple way. For stretching forces such that  $\alpha \geq 2$  the derivative of elongation  $d/dL \langle z(N) \rangle$  does not vary with  $L$  and stays very close to the *constant*  $\langle z(N)/L \rangle_{WLC}$  predicted, for a given force, by the WLC model in absence of spatial constraints. The only modification is the apparition in the elongation of an offset term independent of  $L$ . In more precise words, the elongation  $\langle z(N) \rangle$  can be

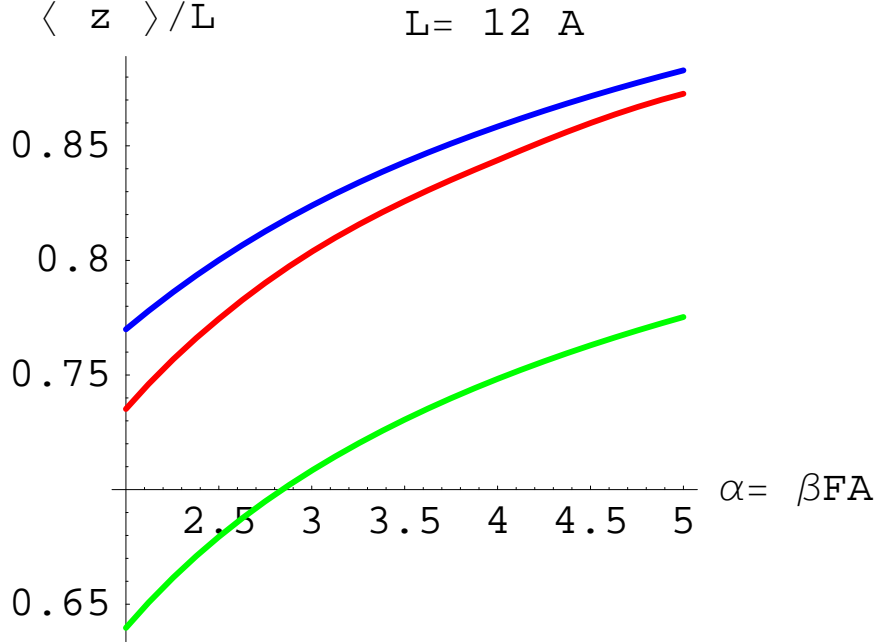


FIG. 3: This figure displays three curves, giving the “short” dsDNA relative elongation versus the stretching force, corresponding to different spatial constraints. Going from top to bottom, the blue curve is the prediction of the WLC model, incorporating both the bead and the anchoring plate spatial obstruction. The red curve accounts for the sole effect of the anchoring plate. The green curve, lying significantly below, has been computed in absence of any spatial constraints. These curves emphasize the dominant role played by the anchoring plate.

written as follows when  $L > 2A$ :

$$\langle z(N) \rangle = L \langle z(N)/L \rangle_{WLC} (1 + \epsilon) + A \Delta_{ofs}(\alpha), \quad (22)$$

where  $|\epsilon| < 10^{-2}$  and the dimensionless offset  $\Delta_{ofs}(\alpha)$  is a slowly decreasing function of  $\alpha$ , which takes values of the order of unity when  $2 \leq \alpha \leq 5$ .

In the present paper, we have performed - within our model - the same analysis in presence of the magnetic bead in thermal equilibrium with the dsDNA. We have also found a linear

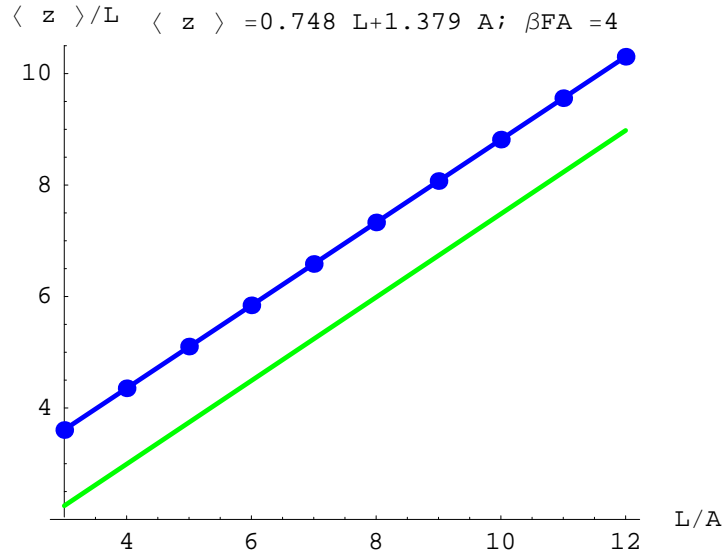


FIG. 4: dsDNA elongation versus contour length, within the interval  $2A \leq L \leq 12A$ . The blue points have been obtained from a version of the WLC model, implementing the magnetic tweezer spatial obstructions. They are well fitted by a straight line (the blue line), having a slope very close to the prediction of the unconstrained WLC model, given by the green line. It is to be noted that the extrapolated fitted line does not pass through the origin, as it should if the corrected elongation were still an extensive quantity. The constant offset term, responsible for this non-extensive behavior, gives rise to a 15% upward shift of the elongation when  $L = 12A$ .

variation of the elongation with respect to  $L$ , similar to that given by equation (22); the only difference is an increase of the offset function  $\Delta_{ofs}(\alpha)$  by a few tens of percents. As an illustration, we have plotted on Fig. 4 the result of a linear fit (the blue line) involving the elongations  $\langle z(N) \rangle$  relative to a given set of contour lengths. They were computed with the method described in section II for  $\alpha = 4$ , when  $L = Nb$  takes 10 equally spaced values within the interval  $2A \leq L \leq 12A$ . The slope coming from the fit coincides, to better than 1%, with the prediction of the unconstrained WLC model, which appears as a green line on Fig. 4. Similar features hold true for the linear elongation fits performed on the results obtained with seven equally spaced values of  $\alpha$  within the interval  $2 \leq \alpha \leq 5$ . Although we have verified the validity of the linear fit for values of  $L > 12A$  and  $\alpha \geq 2$ , it is certainly not valid for  $\alpha \ll 2$ . We have, indeed, found in ref. [13] (section 2.2) that the elongation upward shift contains an extra term  $\propto \sqrt{L}$  when  $0 \leq \alpha \leq 1$ , with a coefficient which exhibits a very steep decrease with  $\alpha$ .



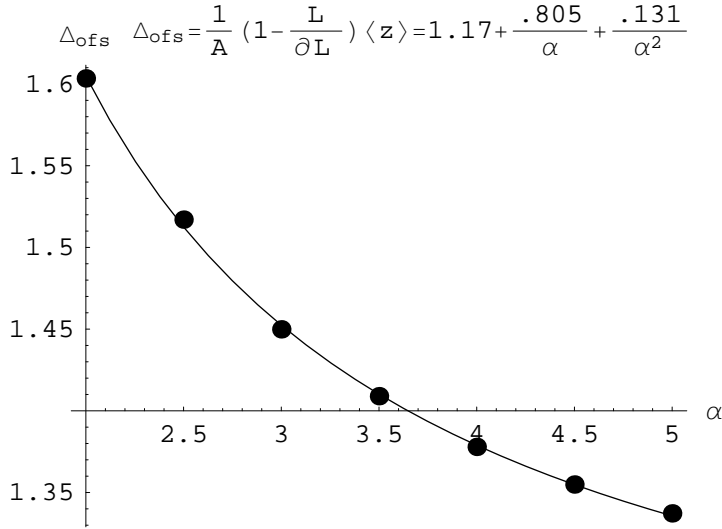


FIG. 5: Numerical values of the offset term  $\Delta_{ofs}(\alpha) = (1 - L/dL) \langle z(L) \rangle / A$  versus seven representative values of  $\alpha$ . A second order polynomial involving  $\alpha^{-1}$  provides a rather accurate interpolation within the interval  $2 \leq \alpha \leq 6$ .

We have plotted on Fig.5 the values of the offset function  $\Delta_{ofs}(\alpha)$  coming from the corresponding elongation linear fits. For the sake of convenience, we have performed a third order polynomial fit, using  $\alpha^{-1}$  as variable:

$$\Delta_{ofs}(\alpha) = 1.6942 + 0.8052 \alpha^{-1} + 0.131213 \alpha^{-2}. \quad (23)$$

No particular physical significance is to be attributed to the functional form chosen for the fit other than the fact it gives a rather simple and accurate interpolation between the calculated values. The formulae (22) and (23), together with the accurate values for  $\langle z(N)/L \rangle_{WLC}$  given in reference [10], lead to a one % evaluation of the dsDNA elongation, corrected for the spatial constraints induced both by the anchoring plate and the magnetic bead. A word of caution: formula (23) is not to be trusted if it is used outside the range  $2 \leq \alpha \leq 5$  and for  $L < 2A$ ; in particular, it does not give the correct limit for  $\alpha \gg 1$  since one expects, on physical ground, that  $\lim_{\alpha \rightarrow \infty} \Delta_{ofs}(\alpha) = 0$ .

## V. THE EMPIRICAL DETERMINATION OF THE PERSISTENCE LENGTH FOR SPATIALLY CONFINED “SHORT” DSDNA MOLECULES.

One may consider that the modification of the dsDNA elongation induced by the magnetic tweezer obstruction effects is, after all, not so dramatic since for the “typical” case  $\alpha = 4$  and  $A/L = 1/12$ , it amounts to an increase of 15%. However, if the elongation together with transverse fluctuation measurements are used to get a determination of the persistence length, the situation becomes much more serious. We would like to show that the raw data of  $\langle z(L) \rangle$ , without a subtraction of the offset correction  $\Delta_{ofs}(\alpha)A/L$ , could lead to totally unreliable values of  $A$ . The basic principle behind this determination of  $A$  is to combine two formulae giving the stretching force  $F$  in terms of  $\langle z(L) \rangle$  and  $\langle x^2(L) \rangle$ : the first one is the Strick *et al.* [5] formula, which is discussed in details in the appendix; the second one is the relation between the reduced force parameter  $\alpha$  and the relative elongation  $u = \langle z(L) \rangle / L$ . In the case of the unconstrained WLC model, it takes a scale invariant form:  $\alpha = \mathcal{F}(u)$ , where  $\mathcal{F}(u)$  is a numerical function, which interpolates accurate numerical results [12]. By a simple algebraic manipulation, one arrives at the relevant formula, valid only within the unconstrained WLC model:

$$A = \frac{\langle x^2(L) \rangle}{\langle z(L) \rangle} \mathcal{F}\left(\frac{\langle z(L) \rangle}{L}\right). \quad (24)$$

It cannot be applied bluntly to the case of “short” DNA molecules studied in the present paper. Let us call  $u_{raw} = \langle z(L) \rangle_{raw} / L$  the relative elongation involving the non-subtracted elongation  $\langle z(L) \rangle_{raw}$ , given in our model by equation (22) and  $A_{raw}$  the corresponding persistence length, obtained by plugging  $u_{raw}$  in equation (24). Ignoring the effect of spatial constraints upon the transverse fluctuations  $\langle x^2(L) \rangle$ , one arrives immediately to the ratio:

$$A_{raw}/A = \frac{u \mathcal{F}(u_{raw})}{u_{raw} \mathcal{F}(u)}. \quad (25)$$

Performing the numerical evaluation for the “typical” case  $\alpha = 4$  and  $A/L = 1/12$ , one gets the rather spectacular result:  $A_{raw}/A = 2.9$ . Such a large number cannot be explained by the finite size correction to the Strick *et al.* formula, estimated in the appendix. It is coming from the fact that  $\mathcal{F}(u)$  exhibits a very sharp increase when  $u \geq 0.75$ , due to the presence of a pole singularity at  $u = 1$ . (See the foot note [12].) If one subtracts from  $u_{raw}$  the offset correction  $\Delta_{ofs}(\alpha)A/L$ , the ratio gets back to a value very close to 1.

If the non-extensive behavior of the elongation has the simple linear behavior described in

the previous section, the required subtraction may be achieved empirically. The procedure involves elongation measurements upon three (or more !) “short” molecules with different contour lengths, say  $L_1 = 5 A$ ,  $L_2 = 10 A$  and  $L_3 = 15 A$ , subjected to the same stretching force. (This latter requirement may be difficult to satisfy with precision.) A linear fit to the data will lead to an empirical determination of  $A \Delta_{ofs}(\alpha)$ , together with a verification of the near equality between the fitted slope and the prediction of the unconstrained WLC model. If the result of the latter test is positive, then one can proceed to the required subtraction from the elongation and plug the result in equation (24). One should get in this way a value of  $A$  close to that obtained for “long” molecules, say with  $L/A \geq 100$ . Finally, the comparison of the empirical value of  $\Delta_{ofs}(\alpha)$  with the prediction given in the previous section will provide a further significant test of our model for the spatial obstruction effects in a magnetic tweezer.

## VI. SUMMARY AND PERSPECTIVES

In the present paper, we have proposed a theoretical model for the spatial-constraint corrections to the dsDNA elasticity measured with a magnetic tweezer. An evaluation of the obstruction effects of the fixed anchoring plate had been given previously [13] and here we have concentrated upon the magnetic bead which is attached to the molecule free end. The main and somewhat unexpected result of this work is that the magnetic bead obstruction effects give rise to a slight upward shift of the elongation, about four times smaller than the anchoring plate effect.

### A. Synopsis of the paper.

- In section II, we have developed theoretical arguments to justify the replacement of the bead surface by its tangent plane at the anchoring point, assumed to be located close to the bead south pole, defined by the force direction. As a first step, we prove, within a discrete version of the WLC model, that the mean square transverse distance between an arbitrary internal “effective” monomer and the anchoring point is smaller than the transverse fluctuations  $\langle x_N^2 \rangle$  of the terminal monomer. This latter quantity is given by the Strick *et al.* formula [5] in terms of the force and the molecular elongation.

Then we proceed, by a simple geometrical argument, to the derivation of a lower bound for the internal monomer mean free path  $\delta_{curv}$  above the tangent plane. For “short” molecules ( $L \lesssim 10 A$ ), stretched by a force  $F \geq 0.3$  pN,  $\delta_{curv}$  is about six times smaller than the root mean square longitudinal fluctuations of the terminal monomer, if the bead radius is larger than one micron. This result suggests strongly that the internal monomers do not really “feel” the bead curvature.

- In section III, we have given a transfer matrix solution of our confinement model, involving a discrete chain of  $N$  effective monomers with the two extremities attached to a pair of parallel repulsive plates. The initial monomer is anchored upon a fixed plate, while the terminal one is stuck to a fluctuating plate, in thermal equilibrium with the attached chain and the ambient fluid. In the first step, the terminal monomer longitudinal coordinate has a fixed value  $z_N$ , taken among a representative set. The partition function of the chain of  $N-1$  fluctuating internal monomers are then obtained by solving, for each fixed value of  $z_N$ , a two-fixed-plate confining model, using the method of ref. [13]. In the second step, we obtain the partition function of the terminal monomer by applying to the last internal monomer the transfer matrix relative to the spatially unconstrained WLC model. The probability distribution of the terminal monomer distribution  $P_N(Z_N)$  exhibits two remarkable features, when it is compared to the same distribution in absence of magnetic bead obstruction. First, the two curves, appearing in Fig. 1 as blue and red continuous lines, are very close. Second, the effect of the bead reduces to a slight upward push given to the terminal monomer. One may have expected naively exactly the reverse: a significant downward push from the “bead”. However, in contrast with the two-fixed-plate problem [13], only the internal monomers feel directly the repulsion from the “bead”, while the terminal monomer stuck on the bead don’t. So, one has to invoke an indirect effect involving the internal monomers. A plausible candidate is the upward pressure they exert on the bead, which is transmitted to the terminal monomer. As long as we are dealing with a small effect, a simple thermodynamic argument leads also to an upward shift of the elongation. We have obtained a qualitative confirmation of the whole picture within the soluble “Gaussian” model, used for flexible polymers. We have found similar effects, but about seven times larger in typical cases. This amplification reflects the

fact that the internal monomers of a flexible polymer, being allowed to move more freely, have larger colliding rates with the “bead”.

- The section IV is devoted to an analysis of the non-extensive behavior of the DNA elongation induced by the magnetic tweezer confinement effects. We have, indeed, found that in DNA molecules, having a contour length  $L \geq 2A$ , the elongation  $\langle z(N) \rangle$  is no longer an extensive quantity, within the force range  $2 \leq \alpha \leq 5$ . The derivative of the elongation with respect to  $L$ ,  $d/dL \langle z(N) \rangle$ , stays very close to the constant value predicted by the unconstrained *WLC* model. The sole non-extensive effect is the apparition in  $\langle z(N) \rangle$  of an offset term  $\Delta_{ofs}(\alpha)A$  independent of  $L$ . In other words, the elongation-versus- $L$  curve is still a straight line but it does not go through the origin. The dimensionless offset term  $\Delta_{ofs}(\alpha)$  decreases slowly from 1.6 to 1.3 within the interval  $2 \leq \alpha \leq 5$  and it is well represented by a second order polynomial in  $\alpha^{-1}$ . For the “typical” case  $\alpha = 4 \rightarrow F = 0.3$  pN and  $A/L = 1/12$ , the non-extensive correction to  $\langle z(N) \rangle/N$  amounts to 15%.
- In the final section, we investigate the possible influence of the magnetic tweezer confinement effects upon the determination of the persistence length  $A$ , from elongation and transverse fluctuations measurements. We consider the case of “short” molecules of about 2 kbp, stretched by a force  $F \simeq 0.3$  pN. Plugging in the basic formula a “raw” relative elongation, uncorrected for non-extensive effects, leads to an overestimate of  $A$  by a factor 3 with respect to “long” molecule values. We suggest an empirical way to perform the required subtraction from the measured elongation.

## B. Possible extension of the present work to super-coiled dsDNA molecules.

In references [27, 28, 29] the WLC model has been generalized to a Rod Like Chain (RLC) Model, involving both bending and twisting rigidities. This makes possible the study of super-coiled dsDNA entropic elasticity below the denaturation threshold.

One can readily modify the RLC model in order to incorporate spatial constraints. The recurrence relation for the partition function  $Z_n(z_n, \theta_n, \kappa)$  relative to a super-coiled DNA molecule, with a given torque  $\Gamma = k_B T \kappa$  acting upon its free end, is obtained by performing in the r.h.s. of the recurrence relation (13) the replacement:  $\mathcal{T}_{WLC}(\theta_{n+1}, \theta_n, f) \rightarrow$

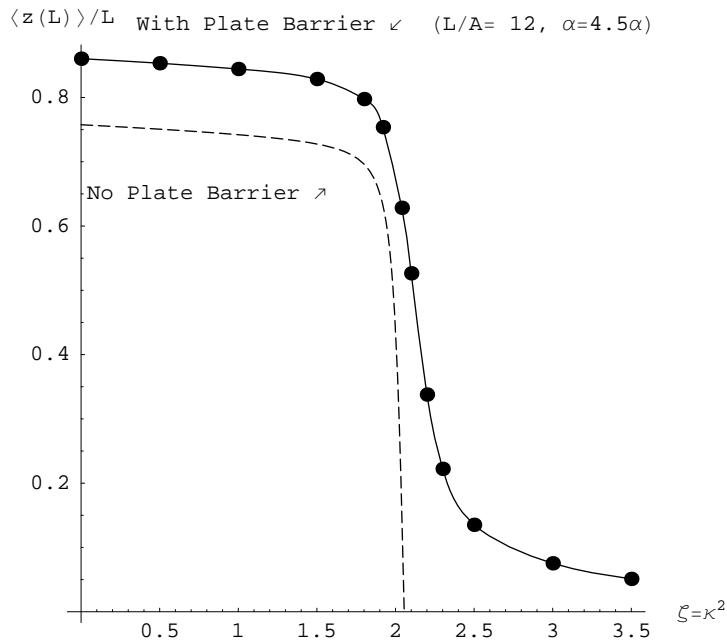


FIG. 6: Two “hat” curves, giving the elongation of a super-coiled molecule versus the torque. The upper curve incorporates the obstruction effects of the anchoring plate, which are ignored in the lower one.

$\mathcal{T}_{RLC}(\theta_{n+1}, \theta_n, f, -\kappa^2)$ , where  $\mathcal{T}_{RLC}$  is given explicitly in ref.[29]. The anchoring-plate barrier is expected to have significant effects upon the so-called “hat curves”, giving, for a fixed force, the relative elongation versus the super-coiling reduced parameter  $\sigma$ . Let us take the “low” force case studied in ref. [28],  $F \simeq 0.1$  pN, where the RLC model “hat curve” dips steeply into the negative  $z$  region when  $|\sigma| \geq 0.03$ . This effect is attributed to the creation of plectonem structures which are allowed to wander in the  $z < 0$  half space, because of the vanishing of their stretching-potential energy. Therefore, we can expect important modifications of the torsion elasticity if the spatial constraints are incorporated in the RLC model.

This effect is illustrated in Fig. 5, which displays the results of a preliminary computation giving the relative elongation  $\langle Z(L) \rangle$  versus the torque  $\Gamma = \kappa k_B T$  for a “short” DNA molecule ( $L/A=12$ ) and  $F = 0.33$  pN. The solid line is a spline fit connecting the points obtained with the RLC model, taking into account the anchoring plate obstruction effects.

The dashed line is relative to the RLC model free of any spatial constraints. The dip of the latter curve into the  $z \leq 0$  half-space reflects the formation of plectonem-like configurations. For  $0 < \kappa < 1$ , the plate barrier effect reduces to an upward shift of the elongation, similar to that found in absence of super-coiling. For  $0 < \kappa < 1$  the anchoring plate confines the molecular chain in the  $z > 0$  half space.

## APPENDIX: CALIBRATION OF THE STRETCHING FORCE FROM ELONGATION AND TRANSVERSE FLUCTUATIONS DSDNA MEASUREMENTS

We would like to use partition function transformation properties under space rotation to derive the Strick *et al.* [5] formula, within the WLC model in the limit where the molecule contour  $L$  is larger than the persistence length  $A$ . This appendix is an updating of an unpublished internal note of the author [11].

The thermal averaging over the various configurations of the molecular chain is performed here within the continuous version of the WLC model, using a technique inspired by quantum mechanics. It leads to the following expression for the partition function:

$$Z(\hat{\mathbf{t}}_0, \hat{\mathbf{t}}_1, \mathbf{F}, L) = \sum_n \Psi_n(\hat{\mathbf{t}}_0 \cdot \hat{\mathbf{z}}) \Psi_n(\hat{\mathbf{t}}_1 \cdot \hat{\mathbf{z}}) \exp\left(-\left(\epsilon_n(\alpha) \frac{L}{A}\right)\right), \quad (\text{A.1})$$

where  $\hat{\mathbf{t}}_0, \hat{\mathbf{t}}_1$  are the unit tangent vectors along the chain at the two ends  $s_0 = 0$  and  $s_1 = L$ ,  $\epsilon(\alpha)$  and  $\Psi_n(\hat{\mathbf{t}} \cdot \hat{\mathbf{z}})$  are respectively eigen-values and eigen-functions of the WLC Hamiltonian  $H_{WLC}$  [30]. The partition function written above is clearly invariant upon simultaneous rotations of  $\hat{\mathbf{t}}_0, \hat{\mathbf{t}}_1$  and  $\mathbf{F}$  but it is modified by rotating  $\mathbf{F}$  while keeping  $\hat{\mathbf{t}}_0, \hat{\mathbf{t}}_1$  fixed or *vice versa*. If the experiments are performed under the condition  $L \gg A$ . it is legitimate to make two simplifications in the right hand side of Eq. (A.1):

i) The sum over  $n$  is dominated by the ground state contribution ( $n = 0$ ), since the excited state contribution is strongly suppressed by a factor of the order of  $\exp(-(\Delta\epsilon_1 L/A))$ , where  $\Delta\epsilon_1 = \epsilon_1 - \epsilon_0 \sim 1$ .

ii) Keeping only the ground state term, the logarithm of the partition function reads as follows:

$$\ln Z(\hat{\mathbf{t}}_0, \hat{\mathbf{t}}_1, \mathbf{F}, L) = -\frac{L}{A} \epsilon_0(\alpha) \left(1 + O\left(\frac{L}{A}\right)\right). \quad (\text{A.2})$$

The term  $O(\frac{L}{A})$  comes from the prefactor involving logarithms of the ground state wave function.

So we can conclude that the free energy of the molecule stays invariant when one rotates the force  $\mathbf{F}$ , while maintaining fixed the two end tangent vectors  $\hat{\mathbf{t}}_0, \hat{\mathbf{t}}_1$ , provided finite size effects of the order of  $\frac{A}{L}$  are ignored.

We are now going to exploit this result by using the path integral form of the partition function:

$$Z(\hat{\mathbf{t}}_0, \hat{\mathbf{t}}_1, \mathbf{F}, L) = \int \mathcal{D}(\hat{\mathbf{t}}) \exp - \left( \frac{E_{bend} + E_{stretch}}{k_B T} \right), \quad (\text{A.3})$$

where  $\mathcal{D}(\hat{\mathbf{t}})$  is the path integral measure and  $E_{bend}$  is the elastic energy describing the resistance against bending. The stretching energy  $E_{stretch}$  is the potential energy associated with the uniform force  $\mathbf{F}$  applied to the free end of the DNA chain:

$$E_{stretch} = -\mathbf{r}(L) \cdot \mathbf{F} = - \int_0^L ds \hat{\mathbf{t}}(s) \cdot \mathbf{F}, \quad (\text{A.4})$$

where  $\mathbf{r}(L)$  is the coordinate of the end point. Instead of taking as usual  $\mathbf{F}$  along the  $z$ -axis, let us apply to  $\mathbf{F}$  a rotation  $\mathcal{R}_y(\delta)$  of angle  $\delta$  about the  $y$ -axis, leaving unchanged  $\hat{t}_0$  and  $\hat{t}_1$ . The stretching energy reads, then, as follows:

$$E_{stretch}(\delta) = -(z(L) \cos \delta + x(L) \sin \delta) F. \quad (\text{A.5})$$

By writing that the Taylor expansion of  $\ln Z(\hat{\mathbf{t}}_0, \hat{\mathbf{t}}_1, \mathbf{F}, L)$  in the vicinity of  $\delta = 0$  vanishes term by term, we shall obtain a set of linear relations involving the moments of  $x(L)$  and  $y(L)$ . Each moment is weighted by powers of  $f = \frac{F}{k_B T}$  such that the relations involve dimensionless quantities. In fact, the relevant relation is obtained by writing:

$$\begin{aligned} \lim_{\delta \rightarrow 0} \frac{1}{Z(\delta)} \frac{\partial^2 Z(\delta)}{\partial \delta^2} &= \lim_{\delta \rightarrow 0} \left\langle \exp \left( \frac{E_{stretch}(\delta)}{k_B T} \right) \frac{\partial^2}{\partial \delta^2} \exp - \left( \frac{E_{stretch}(\delta)}{k_B T} \right) \right\rangle \\ &= f^2 \langle x^2(L) \rangle - f \langle z(L) \rangle, \end{aligned} \quad (\text{A.6})$$

where the r.h.s. has to be understood as a thermal average. If one uses the rotation invariant partition function given by eq. (A.2), the l.h.s of the above equation vanishes, up to corrections of the order of  $\frac{A}{L}$ . One arrives then immediately at the formula of Strick *and al.* [5] which gives the stretching force  $F$  in term of the DNA elongation and the transverse fluctuations of the free end:

$$F = \frac{\langle z(L) \rangle k_B T}{\langle x^2(L) \rangle} \left( 1 + O\left(\frac{A}{L}\right) \right). \quad (\text{A.7})$$

Note that the above derivation does not use any small angle approximation.



We shall try to estimate the correcting terms under conditions such that  $\frac{A}{L}$  is no longer negligible, say  $\frac{A}{L} \sim 0.2$ , while  $\exp(-\frac{L}{A}) \sim 0.007$  is still very small. The simplification i) is still legitimate, so we can use for the partition function the following approximate form:

$$Z(\hat{\mathbf{t}}_0, \hat{\mathbf{t}}_1, \mathbf{F}, L) \simeq \Psi_0(\hat{\mathbf{t}}_0 \cdot \hat{\mathbf{z}}) \Psi_0(\hat{\mathbf{t}}_1 \cdot \hat{\mathbf{z}}) \exp\left(-\epsilon_0(\alpha) \frac{L}{A}\right). \quad (\text{A.8})$$

If we apply the rotation  $\mathcal{R}_y(\delta)$  to the force, the partition function of eq. (A.8) is then  $\propto \Psi_0(\cos(\theta_0 - \delta)) \Psi_0(\cos(\theta_1 - \delta))$ . The computation of the finite size correcting term:  $\Delta_{f.s}(\theta_0, \theta_1) = \lim_{\delta \rightarrow 0} \frac{1}{Z(\delta)} \frac{\partial^2 Z(\delta)}{\partial \delta^2}$  is straightforward, but the final result is rather lengthy. The calibration formula corrected for finite size effects, valid for any value of  $\theta_0$  and  $\theta_1$ , is then readily obtained from eq.(A.6):

$$F = \frac{\langle z(L) \rangle k_B T}{\langle x^2(L) \rangle} \left( 1 + \Delta_{f.s}(\theta_0, \theta_1) \frac{A}{\langle z(L) \rangle \alpha} + O\left(\frac{A^2}{L^2}\right) \right). \quad (\text{A.9})$$

With the above writing, the finite size correction is proportional to  $A/(\langle z(L) \rangle \alpha)$ . We are going now to estimate the prefactor  $\Delta_{f.s}(\theta_0, \theta_1)$ . It is of interest to quote the result in the simple case  $\theta_1 = \theta_0 = 0$  :

$$\Delta_{f.s}(0, 0) = \lim_{\delta \rightarrow 0} \frac{1}{Z(\delta)} \frac{\partial^2 Z(\delta)}{\partial \delta^2} = -2 \frac{\Psi'_0(1)}{\Psi_0(1)}. \quad (\text{A.10})$$

Let us first consider “large” force values :  $\alpha \gg 1$ , remembering that  $\alpha = 4$  corresponds to  $F = 0.3$  pN ! An approximate ground state wave function can be easily derived, together with the corresponding eigen-energy:

$$\Psi_0(\cos \theta) \propto \exp -\frac{1}{2}(\sqrt{\alpha} \theta^2) \quad \text{and} \quad \epsilon_0(\alpha) = -\alpha + \sqrt{\alpha}.$$

It leads immediately to the relative extension:  $\langle z(L) \rangle / L \simeq 1 - \frac{1}{2\sqrt{\alpha}}$  ( this value is very close to the exact one when  $\alpha \geq 4$ ). The correcting term  $\Delta_{f.s}(\theta_0, \theta_1)$  can be computed easily for arbitrary  $\theta_i$  angles:

$$\Delta_{f.s}(\theta_0, \theta_1) = -2\sqrt{\alpha} + \alpha (\theta_0 + \theta_1)^2. \quad (\text{A.11})$$

The above formula shows clearly that something has to be said about the angles  $\theta_0$  and  $\theta_1$ . The angle  $\theta_0$  gives the direction of the initial strand, having a length of about  $0.1 A$ , sticking out from the anchoring plate. The angle is partly determined, first, by the biological gluing process, second, by the fluctuating tension force induced by the rest of the chain. If the latter mechanism were the dominant one, a thermal average would have to be performed, using

the probability distribution  $\propto \Psi_0(\cos \theta_0)$ . A similar analysis holds for the terminal strand, sticking into the magnetic bead. Computing the thermal average  $\langle (\theta_0 + \theta_1)^2 \rangle = 2\langle \theta_0^2 \rangle = 2\sqrt{\alpha}$ , one gets  $\Delta_{f.s}(\theta_0, \theta_1) = 0$ . ( This result turns out to be valid for arbitrary forces. It hinges upon the fact that thermal averaging over  $\theta_0$  and  $\theta_1$  and the second derivative  $\frac{\partial^2}{\partial \delta^2}$  are commuting operators. The latter statement is not totally trivial since the wave function  $\Psi_0(\cos \theta)$  is restricted to the finite interval  $0 \leq \theta \leq \pi$ .) The above considerations lead to the following approximate bounds for the finite size correction:

$$\alpha \gg 1 \Rightarrow -2 \frac{A}{L} \frac{1}{\sqrt{\alpha}} \lesssim F \frac{\langle x^2(L) \rangle}{\langle z(L) \rangle k_B T} - 1 \lesssim 0. \quad (\text{A.12})$$

Let us apply the above result to a situation considered in section II, involving a “short” molecular chain  $A/L = 1/12$  together with a stretching force  $\alpha = 4 \rightarrow F = 0.3$  pN . The large  $\alpha$  asymptotic formulae give already a fair approximation. One sees immediately that the finite size correction stays below the 10 % level, when  $\alpha \geq 4$ .

In the small  $\alpha$  limit, the ground state wave function is obtained by a first order perturbation calculation:

$$\Psi_0(\cos \theta) = \frac{1}{\sqrt{2}}(1 + \alpha \cos \theta + O(\alpha^2)).$$

Performing some simple algebra, one gets:

$$\frac{\langle z(L) \rangle}{L} = \frac{2}{3} \alpha \quad \text{and} \quad \Delta_{f.s}(\theta_0, \theta_1) = -\alpha (\cos(\theta_0) + \cos(\theta_1)) + O(\alpha^2).$$

In the present low force limit the initial and final angle,  $\theta_0$  and  $\theta_1$ , are weakly affected by the tension of the chain. To take into account the spatial constraints associated with the anchoring plate and the magnetic bead we impose the restriction  $0 \leq \theta_i \leq \pi/2$ . We arrive in this way at the following bounds:

$$\alpha \ll 1 \Rightarrow -\frac{3A}{\alpha L} \leq F \frac{\langle x^2(L) \rangle}{\langle z(L) \rangle k_B T} - 1 \leq 0.$$

Let us take as a typical low force case  $\alpha = 1/3 \Rightarrow F \simeq 1/40$  pN. Using the relation  $\langle \cos \theta \rangle = \langle z(L) \rangle / L = 2/9$ , one gets for the average angle between the running tangent vector and the force direction a value of about 1.3 rad. If one takes  $A/L \simeq 1/10$ , the correction can indeed reach values of the order of unity. However, if one deals instead with a “long” molecule with  $L = 300 A$ , as in the experiments analyzed in ref. [10], one gets  $3A/(\alpha L) = 3 \times 10^{-2}$ . The formula (A.7) is then rather accurate, despite the fact that it

was originally derived within a small angle approximation.

- 
- [1] C. Bustamante, Z. Bryant and S. Smith, *Nature* **421**, 423-427 (2003).
- [2] J.F. Allemand, D. Bensimon and V. Croquette, *Curr. Op. Structural Biology* **13**, 266-274 (2003).
- [3] S.B. Smith, L. Finzi and C. Bustamante, *Science* **258**, 1122 (1992).
- [4] T.T. Perkins, S.R. Quake, D.E. Smith and S. Chu, *Science* **264**, 8222 (1994).
- [5] T.R. Strick, J.-F. Allemand, D. Bensimon, A. Bensimon and V. Croquette, *Science* **271**, 1835 (1996).
- [6] A. Revyakin, R. H. Ebright, and T. R. Strick, *Nature Methods*, **2**, 127-138 (2005).
- [7] A. Revyaki, C.Y.L Liu, R.H. Ebright and T.R. Strick *Science* **314**, 1139-1143 (2006)
- [8] M. Fixman and J. Kovac, *J. Chem. Phys.* **58**, 1564 (1973).
- [9] J.F. Marko and E.D. Siggia, *Science* **265**, 506 (1994).
- [10] C. Bouchiat, M.D. Wang, S.M. Block, J.-F. Allemand and V. Croquette, *Biophys. J.* **76**, 409 (1999).
- [11] C. Bouchiat, Internal note LPT.ENS, (1999).
- [12] In ref. [10] the relative elongation  $u = \langle z(N) \rangle / L$  versus  $\alpha = F A / (k_B T)$  is given by:

$$\alpha = \mathcal{F}(u) = u + \frac{1}{4(1-u)^2} - \frac{1}{4} + \mathcal{P}(u),$$

where the polynomial  $\mathcal{P}(u)$  provides an interpolation of the numerical data obtained by solving accurately the Schrödinger equation associated with the WLC model in absence of spatial constraints:

$$\mathcal{P}(u) = -14.17718 u^7 + 39.49944 u^6 - 38.87607 u^5 + 16.07497 u^4 - 2.737418 u^3 - 0.5164228 u^2.$$

- [13] C. Bouchiat, *J. Stat. Mech.* (2006) P03019; arXiv cond-mat/0501171.
- [14] A.C. Maggs, D.A. Huse and S. Leibler *Europhys. Lett.* **8**, 615 (1988).
- [15] G. Gompper and T.W. Burkhardt, *Phys. Rev. A* , 6124 (1989).
- [16] T. W. Burkhardt, *J. Phys A* **26**, L1157-L1162 (1993).
- [17] T. W. Burkhardt, *J. Phys A* **30**, L167-L172 (1997).
- [18] D.J. Bicout and J.T. W. Burkhardt, *J. Phys. A* **34**, 5745 (2001).
- [19] J. Kierfeld and R. Lipovwsky, *J. Phys. A* **38** L155-L161( 2005).

- [20] N. Saito, K. Takahashi and Y. Yunoki, J. Phys. Soc. Japan, **22**, 219-236 (1967)
- [21] Karl L. Fried, J. Chem. Phys. **44**, 1153-1463 (1971).
- [22] H. Yamakawa, in *Helical Wormlike Chains in Polymer Solutions* (Springer-Verlag, New-York, 1997), chapter **3**, 19-47.
- [23] E. Helfand and Y. Tagami, J. Chem. Phys. **56**, 3592-3601 (1971).
- [24] D.C. Morse and G.H. Fredrickson, Phys. Rev. Lett. **73**, 3235 (1994).
- [25] Segall D, Nelson P and Phillips R , Phys. Rev. Lett. **96**, 088306 (2006).
- [26] Jinyu Li, Philip C. Nelson, and M.D. Betterton, Macromolecules **39**, 8816 (2006).
- [27] J.D. Moroz and P. Nelson, Proc. Natl. Acad. Sci. USA **94**, 11418 (1997), Macromolecules **3**, 6333 (1998).
- [28] C. Bouchiat and M. Mézard, Phys. Rev. Lett. **80**, 1556 (1998).
- [29] C. Bouchiat and M. Mézard, Eur. Phys. J.E. **2**, 377-402 (2000).
- [30] The Hamiltonian  $H_{WLC}$  is invariant under rotations around the force direction  $\hat{\mathbf{z}}$ . As a consequence the eigen-functions of  $H_{WLC}$  have the general form:  $\Psi_{n,m}(\hat{\mathbf{t}} \cdot \hat{\mathbf{z}}) \exp(-i m \phi)$  where  $\phi$  is the azimuthal angle of  $\hat{\mathbf{t}}$  around  $\hat{\mathbf{z}}$ . Some readers may wonder why the wave functions with  $m \neq 0$  do not appear in the partition function. The reason is that, in contrast with the case of Quantum Mechanics, the wave function itself has to be interpreted as a probability distribution. The choice  $m = 0$  is then dictated by this physical requirement.